Deep penetration of polycarbonate by a cylindrical punch

S.C. Wright [a], Y. Huang [b] and N.A. Fleck [a]

[a] *Cambridge University Engineering Department, Trunpington Street, Cambridge, CB2 1PZ, UK*
[b] *Division of Applied Sciences, Harvard University, Cambridge, MA 02138, USA*

An experimental and theoretical investigation has been conducted to determine the deep penetration response of polycarbonate (PC). A series of low speed deep penetration tests was performed with steel punches to establish the load versus indentation response, and to enable detailed observation of the penetration processes. The effects of nose shape, lubrication and punch diameter were determined. We found that the average pressure on the indenting end of the penetrator is equal to 4–5 times the tensile yield stress and is independent of nose shape and penetrator diameter. A hackle zone of microcracked material extends to a diameter of 1.4 times that of the penetrator, and this is surrounded by a plastic zone which extends to a diameter of 3.5 times that of the penetrator. A model of deep penetration is developed, based on the assumption that the average pressure on the nose of the penetrator equals the pressure required to expand an infinitely small circular cylindrical void to the diameter of the penetrator. The model assumes the existence of an outer elastic zone, a plastic zone and a hackle zone surrounding the penetrator. The predicted penetration pressure and the diameters of the hackle and plastic zones are reasonably accurate.

1. Introduction

Polycarbonate (PC) is a transparent thermoplastic which is commonly used in lightweight armour, in applications ranging from safety goggles to aircraft windshields. PC possesses an unusually high ballistic resistance to penetration and perforation due to a high ductility and a high strength over a wide range of strain rates and temperature (Fleck et al., 1990). The purpose of the present paper is to quantify the resistance of PC to penetration by circular cylindrical steel punches, and to present a model of penetration.

The paper is in the spirit of the investigation by Bishop et al. (1945) who examined the penetration resistance of ductile metals. Bishop et al. used an elastic–plastic cavity expansion model in order to estimate the indentation resistance of

metals. Polymers differ from metals in showing a limited ductility under uniaxial compressive loading, and in displaying a potent (exponential) strain hardening characteristic. We find that the cavity expansion model is able to predict the penetration pressure provided account is taken of these two factors. Cavity expansion models have been used with success to model the penetration response of soils (Gibson and Anderson, 1961), and the surface indentation response of metals (Johnson, 1970; Fleck et al., 1992). The effect of various hardening laws on the cavitation pressure of cylindrical cavities has been addressed by Durban (1979). Recently, cavitation instabilities have been explored for elastic-power law hardening solids under general axisymmetric loading (Huang et al., 1991).

The structure of the paper is as follows. First, deep penetration tests on PC are reported. The cavitation model is then presented, and the penetration pressure is calculated for a range of material responses; the effects of material hardening

Correspondence to: Dr. N.A. Fleck, University of Cambridge, Department of Engineering, Trunpington Street, Cambridge, CB2 1PZ, UK.

and ductility are predicted. Theoretical predictions are compared with the experimental results, and the accuracy of the model is assessed.

2. Deep penetration tests

Quasi-static deep penetration tests were performed on PC blocks using circular cylindrical hardened steel punches. We varied the nose shape and punch radius a, and measured the force F on the punch as a function of distance penetrated v.

Steel punches of diameter $2a$ in the range 3.5–14 mm were machined with either flat or hemispherical ends. They were driven into blocks of cast PC using a screw driven test machine at an indentation rate of 0.01 mm s^{-1}. The punches were either dry, or lubricated with silicon spray before the test. Bishop et al. (1945) used punches with a cut-back shank to eliminate the friction on the sides of the punch; this geometry was not adopted in the present study as PC exhibits a large elastic spring-back associated with a large yield strain. Load versus indentation plots were recorded, and the evolution of damage was observed. The blocks were approximately 100 mm square and 52 mm deep (the thickest section of polycarbonate available). Two opposing side faces of each block were milled flat, and then polished by hand. This enabled detailed observation and photography of the material around the punch. The polished surfaces were wetted with the pol-

ishing solution during the test to improve clarity. The blocks were supported on their lower faces by the load cell of the machine; the experimental configuration is shown in Fig. 1.

2.1. Results

Typical load versus penetration responses are shown in Figs. 2a and 2b. Figure 2b includes the response for a test using a polymethyl methacrylate (PMMA) specimen. In all cases the response is linear following an initial transient which extends over a penetration depth of approximately 1 punch diameter. A diffuse zone of microcracks forms around the end of the punch, as shown in Fig. 3. The nucleation of each crack gives rise to a load drop in the observed penetration response, see Fig. 2. The indentation interval between successive load drops is less for the PMMA than for the PC. This is due to the smaller fracture strain and lower fracture toughness observed for PMMA (Wright, 1991). Attempts to lubricate the punch were relatively ineffective, and there is little difference between the response with and without lubricant. It is noted that the magnitude of the load drops is greater for the dry punch.

We may deduce the average end pressure acting on the punch $\bar{p}$, and the average frictional shear stress $\bar{\tau}$ on the sides of the punch, as follows. The load P applied by the test machine on the punch can be approximated by
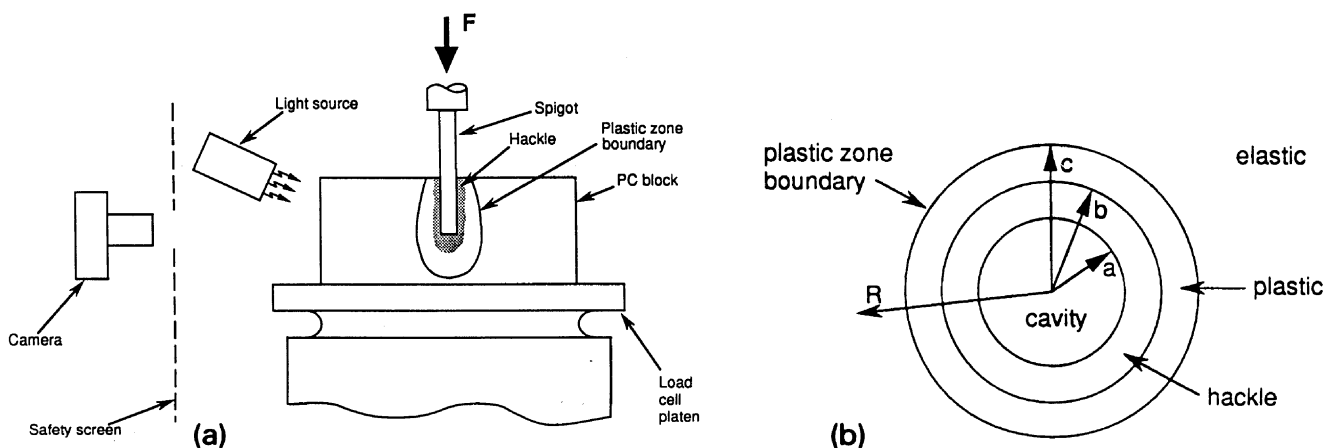
$$P = P_t + P_f, \qquad (2.1)$$

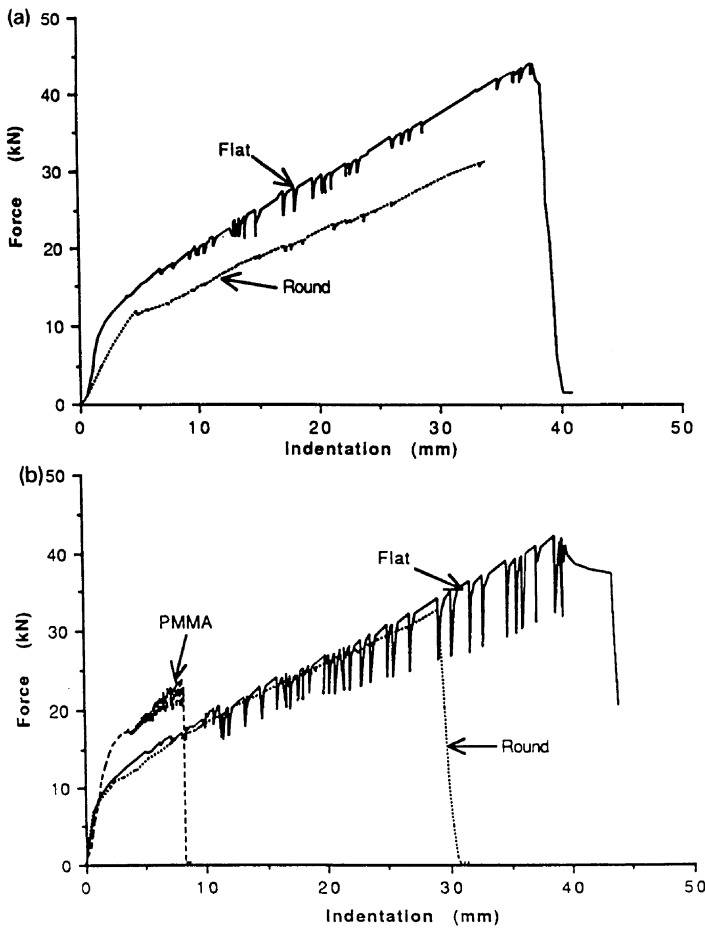Fig. 1. (a) Sketch of the deep penetration test; (b) Idealised cross section of PC after penetration.

Fig. 2 Effect of nose shape on load versus indentation response: (a) 7 mm diameter lubricated punch; (b) 7 mm diameter dry punch. (Response of PMMA is included.)

Fig. 3. Photograph showing diffuse hackle zone surrounding 11.5 mm diameter punch penetrating PC.

where $P_t = \pi a^2 \bar{p}$ is the axial load on the punch tip, and P_f is the load due to friction on the sides of the punch. Assuming that the frictional stress $\bar{\tau}$ on the punch wall is constant we find,

$$P_f = 2\pi a \bar{\tau} v, \qquad (2.2)$$

where v is the penetration depth of the punch. The observation that the load versus penetration depth response is linear supports the assumption of a constant shear stress $\bar{\tau}$. The slope of the P versus v responses give $\bar{\tau} = 26$–30 MPa for PC, which is slightly less than the shear yield stress $\tau_y = 35$ MPa for PC (Fleck and Wright, 1989). For PMMA, $\bar{\tau} = 65$ MPa compared with a shear yield stress of approximately 40 MPa.

The end load P_t on the punch was determined by extrapolating the P versus v response back to zero displacement. The corresponding values of
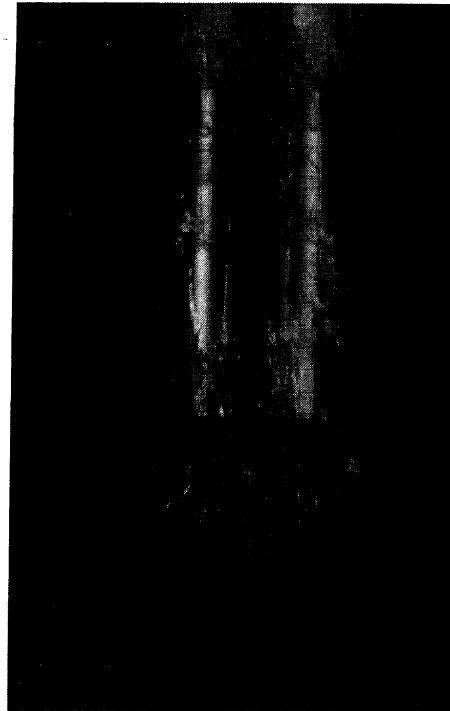
penetration pressure $\bar{p}$ are given in Fig. 4. The average value of $\bar{p}$ for the flat ended punch is 290 MPa or 4.6 times the uni-axial tensile yield stress $\sigma_y = 62.8$ MPa. For the hemi-spherically ended punch the average value of $\bar{p}$ is 270 MPa or 4.3 times the uni-axial tensile yield stress σ_y. These values are close to those observed by Bishop et al. (1945) for the indentation of copper,
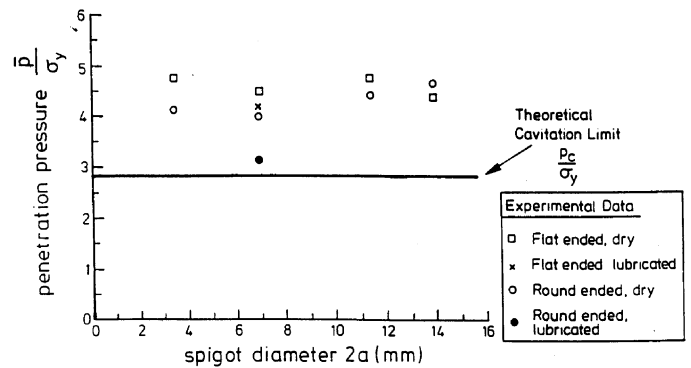

Fig. 4. Measured penetration pressure for PC as a function of punch diameter, $2a$. The theoretical line is the prediction of the cavity model for the uni-axial response observed by Vest et al. (1991) with $\epsilon_f = 0.8$.
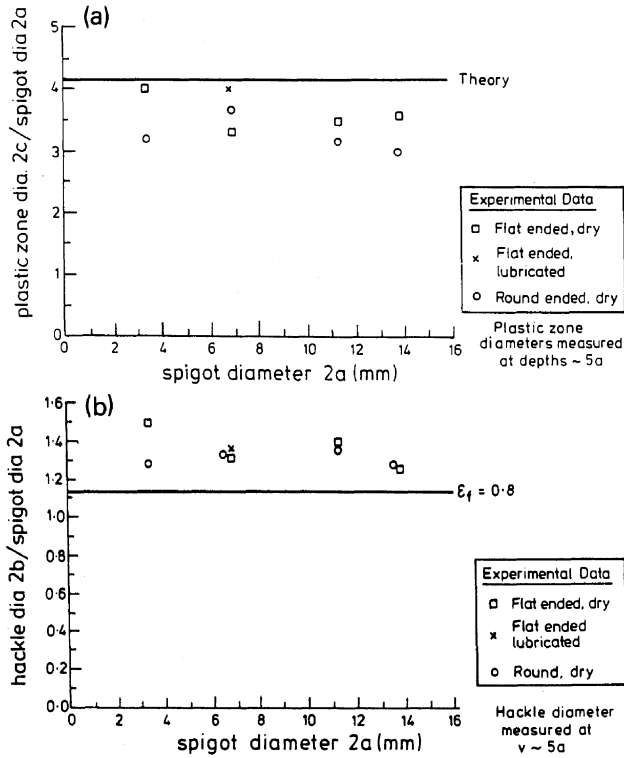
Fig. 5. Effect of punch diameter $2a$ upon: (a) plastic zone diameter $2c$ (the theoretical line is the prediction (3.12) for $\epsilon_y = 0.0345$); (b) hackle diameter $2b$ (the theoretical prediction is given by (3.18) with $\epsilon_f = 0.8$).

where the pressure is about five times the yield stress. The effect of nose shape and lubrication condition on the penetration pressure is small.

The plastic zone and hackle zone diameters were measured from photographs taken through the polished side wall of the specimen. The refractive index of PC changes markedly at yield, enabling measurement of the plastic zone boundary. The plastic zone diameter equals 3.5 times the punch diameter, independent of punch size, nose shape and degree of lubrication, see Fig. 5a. The hackle zone is contained fully within the plastic zone and extends to a diameter of 1.4 times the punch diameter in all cases, as shown in Fig. 5b.

3. Cavitation model

We follow the approach of Bishop et al. (1945) in estimating the average indentation pressure required to advance a cylindrical rod into an elastic–plastic medium. For a frictionless rod indenting a non-linear elastic solid the average

pressure equals the pressure required to expand a cylindrical cavity from zero initial radius to a final radius equal to the radius of the punch. A hemi-spherically shaped false head of PC moves ahead of the tip of the punch, and results in radial displacement of the surrounding material. In the analysis we shall include the effect of a cracked hackle zone surrounding the punch upon the indentation pressure.

Consider the expansion of a circular cylindrical cavity of initial radius a_0 and current radius a in an incompressible elastic–plastic infinite medium. We summarise here the theory developed previously by Hill (1950) and Durban (1979). The cavity is loaded by an internal pressure p. We analyse the axisymmetric problem where straining along the axis of the cylinder equals zero. Since straining is proportional for this problem, flow and deformation theories coincide. In terms of cylindrical polar coordinates, a material point initially at (r, θ, z) moves to a current position (R, θ, z). The solid is taken as an incompressible deformation theory solid such that the logarithmic strain ϵ associated with the Cauchy true stress σ in uni-axial tension is given by

$$\sigma/\sigma_y = f(\epsilon), \quad \epsilon = f^{-1}(\sigma/\sigma_y), \quad (3.1)$$

where σ_y is a representative yield stress. Under general loading the material response is

$$\epsilon_{ij} = \frac{3}{2E}S_{ij} + g(J_2)S_{ij} \quad (3.2)$$

Here, E is Young's Modulus, S_{ij} is the stress deviator, $J_2 = \frac{1}{2}S_{ij}S_{ij}$ and the first term of (3.2) is the elastic strain component; the function $g(J_2)$ is determined from the uni-axial stress strain curve, giving,

$$g(J_2) = \frac{3f^{-1}\left(\sqrt{3J_2}/\sigma_y\right)}{2\sqrt{3J_2}} - \frac{3}{2E}. \quad (3.3)$$

We derive an expression for the pressure p as a function of a/a_0 by integrating the radial equilibrium equation in the current configuration,

$$\frac{\partial \sigma_R}{\partial R} + \frac{1}{R}(\sigma_R - \sigma_\theta) = 0. \quad (3.4)$$

First we express the strain components of each material point in terms of its current radius R. Incompressibility dictates that $\epsilon_R = -\epsilon_\theta$, and

$$R^2 - a^2 = r^2 - a_0^2. \tag{3.5}$$

The strain–displacement relations follow from (3.5) as

$$\epsilon_\theta = -\epsilon_R = \ln\left(\frac{R}{r}\right) = -\frac{1}{2}\ln\left(1 - \frac{a^2 - a_0^2}{R^2}\right). \tag{3.6}$$

On noting that $S_R = -S_\theta = (\sigma_R - \sigma_\theta)/2$, equations (3.2) and (3.3) give, via (3.6),

$$\frac{\sigma_\theta - \sigma_R}{\sigma_y} = \frac{2}{\sqrt{3}}f\left[-\frac{1}{\sqrt{3}}\ln\left(1 - \frac{a^2 - a_0^2}{R^2}\right)\right]. \tag{3.7}$$

We substitute expression (3.7) for $(\sigma_\theta - \sigma_R)$ into the equilibrium equation (3.4), and integrate in order to obtain an expression for p/σ_y as a function of a/a_0, giving

$$\frac{p}{\sigma_y} = \frac{2}{\sqrt{3}}\int_1^\infty f\left[-\frac{1}{\sqrt{3}}\ln\left(1 - \frac{1 - (a_0/a)^2}{\eta^2}\right)\right]\frac{d\eta}{\eta}, \tag{3.8}$$

where $\eta = R/a$.

The above finite strain analysis indicates the existence of a cavitation limit, that is $p \to p_c$ as $a/a_0 \to \infty$, where

$$\frac{p_c}{\sigma_y} = \frac{2}{\sqrt{3}}\int_1^\infty f\left[-\frac{1}{\sqrt{3}}\ln\left(1 - \frac{1}{\eta^2}\right)\right]\frac{d\eta}{\eta}. \tag{3.9}$$

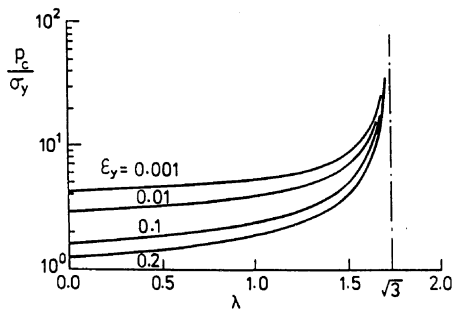
Fig. 6. Effect of hardening exponent λ upon cavitation pressure p_c.

By making the change of variable

$$X = -\frac{1}{\sqrt{3}}\ln\left(1 - \frac{1}{\eta^2}\right),$$

equation (3.9) may be re-written as,

$$\frac{p_c}{\sigma_y} = \int_0^\infty \frac{f(X)}{\exp(\sqrt{3}X) - 1}dX. \tag{3.10}$$

3.1. Predictions for materials of infinite ductility.

Consider an exponential hardening solid, which is representative of the responses of several polymers. A suitable choice of constitutive response is,

$$f(\epsilon) = \begin{cases} \epsilon/\epsilon_y, & \epsilon \leqslant \epsilon_y, \\ \exp[\lambda(\epsilon - \epsilon_y)], & \epsilon > \epsilon_y, \end{cases} \tag{3.11}$$

where λ is the exponential hardening index and the yield strain $\epsilon_y = \sigma_y/E$. The cavitation pressure p_c is calculated from (3.10) and (3.11); it is finite provided $\lambda < \sqrt{3}$. Typical values of p_c are given in Fig. 6 from a numerical integration of equation (3.10). We note that p_c/σ_y increases strongly with increasing λ and with decreasing ϵ_y.

In the cavitation state the plastic zone radius c increases linearly with the void radius a in the deformed configuration. At the edge of the plastic zone $\sigma_\theta - \sigma_R = \sigma_y$ and $f(\epsilon_y) = 1$, thus (3.7) gives in the limit of $a/a_0 \to \infty$,

$$c/a = \left[1 - \exp\left(-\sqrt{3}\epsilon_y\right)\right]^{-1/2}. \tag{3.12}$$

We note that c/a is independent of the shape of $f(\epsilon)$ beyond yield.

3.2. Cavitation limit for a solid of finite ductility

Engineering metals and polymers fail at finite strains. We shall show that this can have a dramatic effect on the cavitation pressure. PC exhibits distributed micro-cracking in a zone surrounding the penetrator but contained within the plastic zone. A significant proportion of the cracks are in the radial direction. This suggests that we

may treat the cracked hackle zone surrounding the penetrator by a zone in which the hoop stress σ_θ vanishes. Further, we assume that the boundary of the hackle zone at $R = b$ is located by the condition

$$\epsilon_e = \epsilon_f, \tag{3.13}$$

where $\epsilon_e = \sqrt{\frac{2}{3}\epsilon_{ij}\epsilon_{ij}}$ is the effective strain.

Equilibrium within the hackle zone dictates $\sigma_R = -pa/R$ via (3.4) with $\sigma_\theta = 0$. Outside the hackle zone the effective stress $\sigma_e = \frac{1}{2}\sqrt{3}(\sigma_\theta - \sigma_R)$ follows from (3.7) as

$$\frac{\sigma_e}{\sigma_y} = f\left[-\frac{1}{\sqrt{3}}\ln\left(1 - \frac{a^2 - a_0^2}{R^2}\right)\right]. \tag{3.14}$$

We deduce the position of the boundary of the hackle zone by noting that $\sigma_e/\sigma_y = f(\epsilon_f)$ at $R = b$, which gives, from (3.14)

$$\epsilon_f = -\frac{1}{\sqrt{3}}\ln\left(1 - \frac{a^2 - a_0^2}{b^2}\right). \tag{3.15}$$

The pressure in the cavity p is deduced by integration of the equilibrium equation (3.4) as before, which gives via (3.7)

$$\frac{p}{\sigma_y} = \frac{b}{a}\frac{2}{\sqrt{3}}$$

$$\times \int_{b/a}^\infty f\left[-\frac{1}{\sqrt{3}}\ln\left(1 - \frac{1 - (a_0/a)^2}{\eta^2}\right)\right]\frac{d\eta}{\eta}, \tag{3.16}$$

where $\eta = R/a$, and b/a is given by (3.15). At the cavitation limit $a/a_0 \to \infty$, and equations (3.15) and (3.16) combine to give

$$\frac{p_c}{\sigma_y} = \left[1 - \exp(-\sqrt{3}\,\epsilon_f)\right]^{-1/2}$$

$$\times \int_0^{\epsilon_f} \frac{f(X)}{\exp(\sqrt{3}\,X) - 1}\,dX, \tag{3.17}$$

where we have again made the change of variable

$$X = -\frac{1}{\sqrt{3}}\ln\left(1 - \frac{1}{\eta^2}\right),$$

for convenience. The boundary of the hackle zone at the cavitation limit follows from (3.15) as

$$b/a = \left[1 - \exp(-\sqrt{3}\,\epsilon_f)\right]^{-1/2} \tag{3.18}$$

and the edge of the plastic zone is given by (3.12) as before.

The effect of ductility ϵ_f upon the cavitation pressure p_c and upon the hackle zone size is shown in Figs. 7a and 7b, respectively. The cavitation pressure is sensitive to the magnitude of ϵ_f for $\lambda > 1$. For example when $\lambda = 1.6$, p_c/σ_y decreases from 7.8 to 2.1 as ϵ_f decreases from infinity to unity. The radius of the hackle zone decreases with increasing ϵ_f as expected; for $\epsilon_f > 1$, b/a is less than 1.1 for all values of λ.

3.3. Cavitation pressure for polycarbonate

The cavitation pressure for PC has been estimated using an idealised version of the measured uni-axial true stress versus logarithmic strain response of the material (Vest et al., 1987), see Fig. 8a. Vest et al. (1987) observed brittle fracture at a tensile strain of 0.8. An extrapolation of the data of Vest et al. (1987) for $\epsilon > 0.8$ is included in Fig.
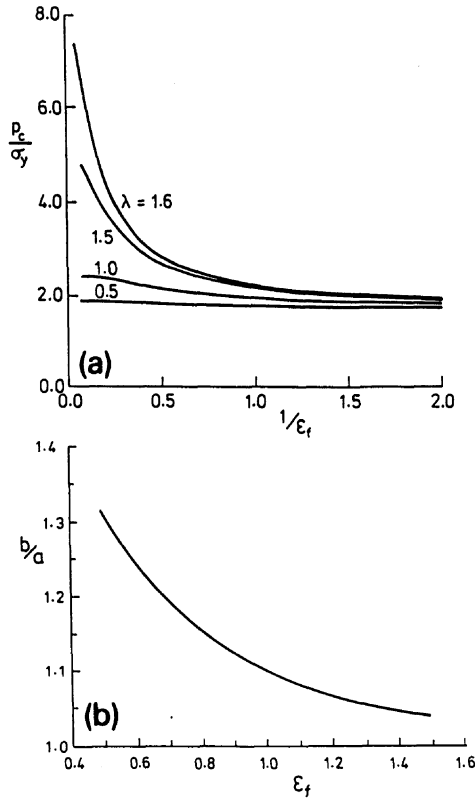
Fig. 7. Effect of true strain to failure ϵ_f upon: (a) the cavitation pressure for an exponential hardening solid ($\epsilon_y = 0.1$); (b) hackle radius b.
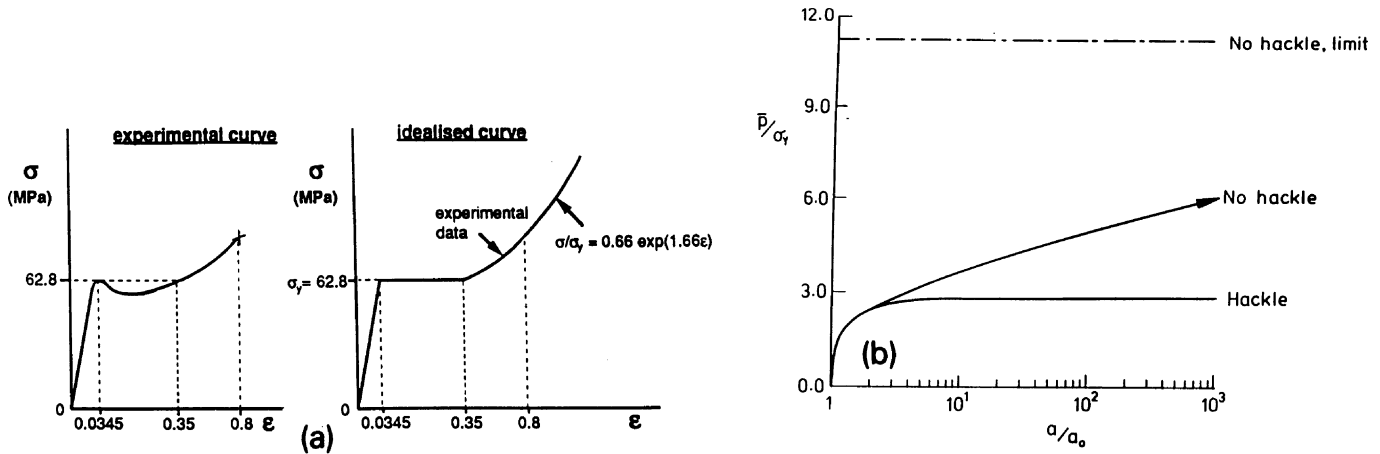
Fig. 8. (a) Approximation to experimental Cauchy stress versus logarithmic strain response used in cavitation model (data taken from Vest et al. (1987); the figure is not drawn to scale); (b) Effect of hackle on evolution of cavitation pressure for PC.

8a. The evolution of cavity pressure p with increasing a/a_0 is shown in Fig. 8b for PC, where we have used the idealised tensile response and have considered two cases $\epsilon_f = 0.8$ and $\epsilon_f = \infty$. We note that the presence of hackle has a dramatic effect upon the cavitation response. For the case of $\epsilon_f = \infty$, p_c/σ_y increases to the value 11.2 over many decades of a/a_0. In the case of $\epsilon_f = 0.8$, p_c/σ_y increases rapidly to the cavitation limit $p_c/\sigma_y = 2.82$, as shown in Fig. 8b.

3.4. Comparison with cavitation model

The predictions of the cavitation model are included in Figs. 4 and 5, where we use the idealised uni-axial response of Vest et al. (1987) in the cavitation model. The cavitation model suggests $\bar{p} = 2.82\sigma_y$ assuming a measured fracture strain of $\epsilon_f = 0.8$, and $\bar{p} = 11.2\sigma_y$ for infinite ductility. The measured value of $\bar{p}$ is $4.5\sigma_y$. We deduce that the presence of hackle significantly reduces the penetration pressure, but the cavitation model with hackle overestimates this effect. The model assumes that the hoop stress vanishes within the hackle zone, and that no redundant plastic work occurs due to non-proportional loading. These two simplifing assumptions lead to an underestimate of the penetration pressure.

Figures 5a and 5b indicate that the model achieves an encouraging prediction for the sizes of the hackle and plastic zones. The slight underestimate of the hackle zone size is probably caused by the failure to model the hoop stress inside the hackle zone accurately.

References

Bishop, R.F., R. Hill and N.F. Mott (1945), The theory of indentation hardness tests, Proc. Phys. Soc. 57, 147–159.

Durban, D. (1979), Large strain solution for pressurised elasto/plastic tubes, J. Appl. Mech. 46, 228–230.

Fleck, N.A. and S.C. Wright (1989), Deformation and fracture of polycarbonate at high strain rate, in: J. Harding, ed., Mechanical Properties of Materials at High Rates of Strain, Institute of Physics Conf. Series No. 102, p. 73.

Fleck, N.A., W.J. Stronge and J.H. Liu (1990), High strain rate shear response of polycarbonate and polymethyl methacrylate, Proc. R. Soc. A429, 459.

Fleck, N.A., H. Otoyo and A. Needleman (1992), Indentation of porous solids, Int. J. Solids Struct. 29(13), 1613–1636.

Gibson, R.E. and W.F. Anderson (1961), In situ measurement of soil properties with the pressuremeter, Civ. Eng. Public Works Rev. 56, 615.

Hill, R. (1950), The Mathematical Theory of Plasticity, Oxford University Press, London.

Huang, Y., J.W. Hutchinson and V. Tvergaard (1991), Cavitation instabilities in elastic–plastic solids, *J. Mech. Phys. Solids 39*, 223–242.

Johnson, K.L. (1970), The correlation of indentation experiments, *J. Mech. Phys. Solids 18*, 115.

Vest, T.A., J. Amodeo and D. Lee (1987), Modelling of tensile stress strain behaviour in semi-crystalline and amorphous polymers, *Constitutive Modelling of Non-Traditional Materials*, Winter Meeting of ASME, Boston, December 13–18, pp. 71–86.

Wright, S.C. (1991), High strain rate response and ballistic impact of polycarbonate, Ph.D. Thesis, Cambridge University.